THE JOURNAL OF BIOLOGICAL CHEMISTRY VOL. 289, NO. 6, pp. 3811–3824, February 7, 2014
Published in the U.S.A.

# A Missense Mutation in *Rev7* Disrupts Formation of Polζ, Impairing Mouse Development and Repair of Genotoxic Agent-induced DNA Lesions*

Received for publication, August 29, 2013, and in revised form, December 13, 2013 Published, JBC Papers in Press, December 19, 2013, DOI 10.1074/jbc.M113.514752

**Maryam Khalaj[‡§1], Abdolrahim Abbasi[‡§1,2], Hiroshi Yamanishi[‡], Kouyou Akiyama[¶], Shuso Wakitani[‡], Sotaro Kikuchi[‖], Michiko Hirose[**], Misako Yuzuriha[**], Masaki Magari[‡], Heba A. Degheidy[‡‡], Kuniya Abe[**], Atsuo Ogura[**], Hiroshi Hashimoto[‖3], and Tetsuo Kunieda[¶4]**

*From the [‡]Graduate School of Natural Science and Technology and [¶]Graduate School of Environmental and Life Science, Okayama University, Tsushima-naka, Okayama 700-8530, Japan, [§]Laboratory of Cellular and Developmental Biology, NIDDK, National Institutes of Health, Bethesda, Maryland 20892, [‖]Graduate School of Nanobioscience, Yokohama City University, Tsurumi-ku, Yokohama 230-0045, Japan, [**]RIKEN Bioresource Center, Koyadai, Tsukuba 305-0074, Japan, and [‡‡]Food and Drug Administration, Division of Biology, Silver Spring, Maryland 20993*

**Background:** *Rev7* encodes a subunit of Polζ for translesion DNA synthesis (TLS).
**Results:** We found a *Rev7* mutation in mice that causes developmental defects and increases susceptibility for genotoxicity.
**Conclusion:** *Rev7* is essential for mouse development through its function in cell proliferation.
**Significance:** These findings demonstrate a unique function of Polζ in development that is absent in other TLS polymerases.

***Repro22* is a mutant mouse produced via *N*-ethyl-*N*-nitrosourea-induced mutagenesis that shows sterility with germ cell depletion caused by defective proliferation of primordial germ cells, decreased body weight, and partial lethality during embryonic development. Using a positional cloning strategy, we identified a missense mutation in *Rev7/Mad2l2* (*Rev7*$^{C70R}$) and confirmed that the mutation is the cause of the defects in *repro22* mice through transgenic rescue with normal *Rev7*. *Rev7/Mad2l2* encodes a subunit of DNA polymerase ζ (Polζ), 1 of 10 translesion DNA synthesis polymerases known in mammals. The mutant REV7 did not interact with REV3, the catalytic subunit of Polζ. *Rev7*$^{C70R/C70R}$ cells showed decreased proliferation, increased apoptosis, and arrest in S phase with extensive γH2AX foci in nuclei that indicated accumulation of DNA damage after treatment with the genotoxic agent mitomycin C. The *Rev7*$^{C70R}$ mutation does not affect the mitotic spindle assembly checkpoint. These results demonstrated that *Rev7* is essential in resolving the replication stalls caused by DNA damage during S phase. We concluded that *Rev7* is required for primordial germ cell proliferation and embryonic viability and development through the translesion DNA synthesis activity of Polζ preserving DNA integrity during cell proliferation, which is required in highly proliferating embryonic cells.**

The arrest of DNA replication after nucleotide damage disrupts the cell cycle and causes genome instability and cell death. Cells can relieve arrest through translesion DNA synthesis (TLS)[5] that provides tolerance to DNA damage (1, 2). In processing damaged DNA through this mechanism, a nucleotide opposite the lesion is incorporated to bypass the damage but at the cost of increased rates of mutation (3, 4). Unlike classic DNA polymerases, many TLS DNA polymerases are present in most human cells (5, 6). One, DNA polymerase ζ (Polζ), is a member of the B family of DNA polymerases and consists of a catalytic and an accessory subunit encoded by *Rev3* (official name, *Rev3l*) and *Rev7* (official name, *Mad2l2* for mitotic spindle assembly checkpoint protein MAD2B), respectively. Polζ has been documented to play a particularly important role in TLS, which is required for DNA repair, recombination, and chromosome stability (1, 7–10).

In yeast, a strong epistatic relationship occurs between *Rev3* and *Rev7* mutations, enhancing susceptibility to genotoxic agents. Although these functions are conserved in vertebrates, studies using cultured cells with defects of these genes document greater complexity (11–13). In addition, a null *Rev3* mutation in mouse results in severe early developmental lethality, leaving its function, especially its involvement in various cell lineages, largely unknown (14–16). A more restricted conditional null mutation of *Rev3* in mouse embryonic fibroblast cells and adult B cells documents a need for Polζ, without which increased chromosomal aberrations lead to enhanced tumorigenesis (17, 18), reduced somatic mutations, and cell proliferation (3, 19). Although overexpression of *REV7* is associated

* This work was authored, in whole or in part, by National Institutes of Health staff. This work was supported in part by grants from the Japan Society for the Promotion of Science.
[1] Both authors contributed equally to this work and are joint first authors.
[2] To whom correspondence may be addressed: Laboratory of Cellular and Developmental Biology, NIDDK, National Institutes of Health, Bethesda, MD 20892. E-mail: abbasiar@mail.nih.gov.
[3] Present address: School of Pharmaceutical Sciences, University of Shizuoka,Yada, Shizuoka 422-8526 Japan.
[4] To whom correspondence may be addressed: Graduate School of Environmental and Life Science, Okayama University, Tsushima-naka 1-1-1, Okayama 700-8530, Japan. E-mail: tkunieda@cc.okayama-u.ac.jp.

[5] The abbreviations used are: TLS, translesion DNA synthesis; APC, anaphase promoting complex; BAC, bacterial artificial chromosome; DSB, DNA double-strand break; FA, Fanconi anemia; ICL, interstrand cross-link; γH2AX, phosphorylated histone H2AX; MEF, mouse embryonic fibroblast; PGC, primordial germ cell; PN, pan-nuclear; Polζ, DNA polymerase ζ; RFLP, restriction fragment length polymorphism; PCNA, proliferating cell nuclear antigen.

with high mortality in patients with colon cancer (20), relatively little is known about the role of *REV7* and its regulation of Polζ function in TLS.

REV7/MAD2L2 is also homologous to the cell cycle checkpoint protein MAD2, and the two proteins share common HORMA domains. The MAD2 protein is a key component of the mitotic spindle assembly checkpoint as an inhibitor of anaphase promoting complex (APC), a surveillance mechanism that delays anaphase until all chromosomes are properly aligned on the metaphase plate (21, 22). Several reports have described the function of Mad2l2 in cell cycle regulation, and mammalian epithelial cells infected by *Shigella* show cell cycle arrest secondary to disruption of Mad2l2 with $APC^{cdh1}$ (23), which suggests that *Rev7*/*Mad2l2* might regulate the cell cycle by interacting with APC.

Herein, we report a unique function of *Rev7* in mouse development and DNA repair using a mouse model of infertility produced by a project known as ReproGenomics at The Jackson Laboratory (24). *Repro22* mice are useful for studying the mechanism of mouse primordial germ cells (PGCs), as both males and females are sterile with a lack of PGCs. Interestingly, the mutant mice display severe embryonic lethality and reduced embryonic body weight. Using positional cloning, we identified a missense mutation in the N terminus of *Rev7* (C70R) that disrupts *Rev7* interaction with *Rev3*. In the absence of Polζ activity, cells become hypersensitive to interstrand cross-link (ICL) damaging agents and accumulate double-stranded breaks (DSBs) in their DNA. We next showed that *Rev7* function is essential to resolving the replication stall in S phase of the cell cycle. Our results show that *Rev7* is required for PGC proliferation and embryonic viability and development through the TLS activity of Polζ to preserve DNA integrity during cell proliferation, which is required in highly proliferating embryonic cells.

## EXPERIMENTAL PROCEDURES

*Mice and Histological Preparations*—The heterozygous *repro22*/+ mice were obtained from The Jackson Laboratory, and the line was maintained through sib mating. The JF1/Ms mice were obtained from the National Institute of Genetics, Mishima, Japan. The *repro22*/+ heterozygous mice were crossed to JF1/Ms mice to generate $F_1$ mice. The $F_1$ mice carrying the mutant allele were intercrossed to generate $F_2$ progeny. Congenic mouse lines were constructed by backcrossing heterozygous mice to C3H mice for 9 generations. Affected and normal mice were classified by the weight of their testes and ovaries. Mice were euthanized, and tissues were excised and fixed by immersion in Bouin's fluid. After dehydration, tissues were embedded in paraffin wax and sectioned. After deparaffination in xylene, sections were rehydrated and stained with Mayer's hematoxylin and eosin. Experimental procedures were approved by the animal care committee of Okayama University.

*Alkaline Phosphatase Staining*—The concepti used in this study were obtained by mating *repro22*/+ male and female mice. Noon on the day of vaginal plug identification was defined as embryonic day 0.5 (E0.5), and pregnant females were euthanized on days E7.5, E8.5, E9.5, E10.5, E11.5, E12.5, and E13.5. For whole-mount preparations, embryos were removed from decidua in phosphate-buffered saline (PBS) and fixed in 4% paraformaldehyde in PBS for 2 h at 4 °C, rinsed in PBS, placed in 70% ethanol for 2–3 h at 4 °C, washed with distilled water, and processed as whole mounts for alkaline phosphatase staining (28, 29). The embryos were stained at room temperature for 10 min with Fast Red TR salt Sigma; F8764) and -naphthyl phosphate (Sigma; 71090) and α-naphthyl phosphate containing 5% borax Sigma; F8764) and 10% $MgCl_2$ in the staining solution. To obtain serial sections, we fixed the embryos in 4% paraformaldehyde and dehydrated them ethanol and xylene before embedding them in paraffin. The sections (7 μm) containing gonads were stained with NBT-BCIP (Boehringer DIG labeling detection kit).

*Linkage Mapping and Mutation Detection*—Genomic DNA was isolated from the tails of 1511 progeny with phenol/chloroform extraction, and fine mapping of the *repro22* locus was performed using polymorphic microsatellite markers on mouse chromosome 4 (Table 1). These markers were genotyped as described previously (25).

For mutation detection, total RNA of the affected and normal animals was extracted from liver, testis, lung, spinal cord, and inner ear tissues using TRIzol reagent (Invitrogen) according to manufacturer instructions. After complementary DNA (cDNA) synthesis using random hexamers and Superscript III reverse transcriptase (Invitrogen), the entire coding regions of five candidate genes were amplified from the cDNAs of affected and normal mice. Primers designed to amplify the open reading frame of *Rev7* messenger RNA are listed in Table 1. Purified polymerase chain reaction (PCR) products were cloned into pGEM-T Easy vector (Promega, Madison, WI) and sequenced using the dye-terminator method with an ABI 3100 sequencer (Applied Biosystems, Foster City, CA). The DNA sequences of normal and affected mice were compared. After identifying the missense mutation in *Rev7*, we designed primers to amplify a 239-bp fragment that contained it (see Table 1) to genotype the mutation with BstUI PCR-restriction fragment length polymorphism (RFLP).

*Transgenic Rescue Experiments*—To identify conserved genomic regions of *Rev7* that may include potential regulatory regions of the gene, we performed a comparative analysis between mice and humans using VISTA (26). The BAC clone RP24–193K16 containing *Rev7* and three other genes was digested using ClaI restriction enzyme to isolate a 24.8-kb fragment containing the entire *Rev7* gene including 5 kb of the potentially regulatory 5′ region and 3 kb of the 3′ untranslated region of the gene and part of the BAC vector. Transgenic mice were generated via intracytoplasmic sperm injection-mediated transgenesis (27). Oocytes were obtained through mating (C57BL/6J × C3H/HeJ) of $F_1$ females and C3H/HeJ males and injected with the BAC fragment containing the intact copy of normal *Rev7*. Transgenic mice were identified with PCR using primers specific to the BAC vector sequence in the fragment (ATCCGGCGCGCCAATAGTCATGCC and CCCTATAGTGAGTCGTATTAGC) that amplified a 130-bp fragment. The transgenic founders with multiple copies of the normal *Rev7* transgene ($Rev7^{TG}$) were crossed with *repro22*/+ females, and the resulting $Rev7^{TG/+}$;*repro22*/+ offspring were crossed to

establish *Rev7*$^{TG/+}$;*repro22*/*repro22* mouse lines. The genotype of the endogenous *Rev7* was determined using genotypes of two flanking microsatellite markers (*D4Mok8* and *D4NIMr1*) as well as PCR-RFLP for the mutation site. The presence of *Rev7*$^{TG}$ was determined with PCR of the BAC vector sequence and Southern hybridization.

*Expression Analysis of Rev7 in Developing PGCs*—We examined the expression of *Rev7* in PGCs isolated from mouse embryos via fluorescence-activated cell sorting (FACS) of β-galactosidase-expressing cells (30). Total RNA was extracted using TRIzol reagent (Invitrogen) and treated with DNase I. The first-strand cDNA was synthesized from the RNA template with reverse transcription using Superscript III reverse transcriptase with oligo-dT primers (Invitrogen). The expression of *Rev7* was examined using semiquantitative reverse transcription-PCR.

*In Vitro Interaction Assay*—cDNA encoding human REV7 and REV3 fragments (residues 1847–1898) was inserted into a pETDuet-1 vector (EMB Millipore, Billerica, MA). The resultant plasmids encoded REV7 with an N-terminal hexameric His tag and the REV3 fragment (31). The C70R substitution of REV7 was introduced via the QuikChange protocol (Agilent, Santa Clara, CA). For the *in vitro* interaction assay between REV7 and the REV3 fragments (32), His-tagged REV7 or *Rev7*$^{C70R}$ mutant protein was co-expressed with the REV3 fragments in *Escherichia coli* BL21(DE3). The cell lysate was applied to $Ni^{2+}$-Sepharose resin (GE Healthcare) in buffer (50 mM HEPES-NaOH, pH 7.4, 500 mM NaCl, and 20 mM imidazole). After washing with buffer (50 mM HEPES-NaOH, pH 7.4, 1.5 M NaCl, and 20 mM imidazole) bound proteins were analyzed using sodium dodecyl sulfate polyacrylamide gel electrophoresis with Coomassie Brilliant Blue staining.

*Assay for DNA Damage Sensitivity*—Mouse embryonic fibroblasts (MEFs) were isolated from E14.5 embryos obtained from interbred *repro22*/+ mice. After removal of the head and intestinal organs, each embryo was minced and digested with trypsin (PBS, 0.05% trypsin, 0.04% EDTA) at 37 °C. The cells were seeded in 100-mm culture dishes (passage 0). MEFs were cultured in 5% $CO_2$ at 37 °C in Dulbecco's modified Eagle's medium (DMEM; Invitrogen) supplemented with 10% fetal bovine serum (FBS; Hyclone Laboratories, Logan, UT), and experiments were performed with early passage MEFs. Cytotoxic and cytostatic effects of DNA damage were assayed via examination of the viability rate of MEFs or the proliferation activity in microculture tetrazolium assays using a CellTiter 96® Aqueous One Solution Assay (Promega) according to manufacturer instructions. Briefly, early passage (2–3) MEFs were seeded into 96-multiwell plates ($5 \times 10^3$ cells/well) and cultured in DMEM with 10% FBS. Three hours later, the percent of viable MEFs in the reference wells of each genotype was determined as the 0-h time point. After an additional 24 h, cells were treated with the indicated concentrations of mitomycin C (Sigma), and their proliferation activity was determined 48 h later.

*Flow Cytometric Analysis of Mitomycin C-treated Cells*—*Rev7*$^{C70R/C70R}$, *Rev7*$^{C70R/+}$, and normal cells ($3 \times 10^5$ cells) were cultured in 10 ml of DMEM containing 10% FBS to adhere in a 10-cm dish. On day 1 of the culture, adhered cells were treated with 1.0 μg/ml mitomycin C (Sigma) for 18 h. After washing with PBS 3 times to remove mitomycin C, cells were cultured for an additional 48 h in 10 ml of fresh culture medium. For estimating the frequency of phosphorylated histone H2AX (γH2AX)-positive cells, MEFs that were cultured for 0 or 48 h after mitomycin C treatment were harvested using 0.025% trypsin, 0.04% EDTA in PBS. These cells were stored in 70% ethanol at −20 °C until staining for FACS analysis.

For flow cytometric analysis, cells were fixed with 3.7% formalin in PBS for 10 min, permeabilized with 0.1% Triton-X, 1% bovine serum albumin (BSA) in PBS for 20 min, and then blocked with 3% BSA in PBS for 30 min at room temperature. The cells were stained with anti-γH2AX (clone: JBW301, Millipore) followed by goat anti-mouse IgG-Alexa-488 (Invitrogen) in PBS and 3% BSA. After washing in PBS twice, the cells were counterstained with propidium iodide (50 μg/ml; Sigma) in PBS containing RNase (10 μg/ml). The frequency of γH2AX-positive cells in each population was estimated on FACS Calibur (BD Biosciences) and Flowjo software (Tree Star, Ashland, OR) according to Huang and Darzynkiewicz (33).

*Spindle Checkpoint Assembly Function Assessment*—*Rev7*$^{C70R/C70R}$ mutant, *Rev7*$^{C70R/+}$, and normal primary MEFs were treated with colcemid and harvested hourly for 8 h. The cells were fixed with 70% ethanol permeabilized with 1% BSA and 0.1% Triton X-100 in PBS containing 0.1% mg/ml RNase. The cells were then stained with Alexa Fluor 488 antibody recognizing phosphorylated histone H3 (Cell Signaling Technology, Beverly, MA) and stained with propidium iodide as described above. The ratio of phosphohistone H3 (Ser-10)-positive cells to total cells was recorded as the mitotic index.

*Terminal Deoxyribonucleotidyltransferase-mediated 2′-Deoxyuridine,5′-triphosphate-digoxigenin Nick End Labeling (TUNEL) and Proliferating Cell Nuclear Antigen (PCNA) Assay*—*Rev7*$^{C70R/C70R}$ cells were seeded in a 16-well glass chamber slide at $5 \times 10^3$ cells/well. After 24 h of seeding, cells were treated with the indicated concentrations of mitomycin C for 18 h. Cells were washed with PBS and further cultured in fresh medium for 48 h. MEFs were then fixed with 3.7% formaldehyde in PBS for 5 min and permeabilized with 0.25% Triton-X in PBS for 5 min at room temperature. Apoptotic cells were detected with TUNEL assay using an In Situ Cell Death Detection kit, POD (Roche Diagnostics). After the TUNEL assay, preparations were counterstained with 4′,6-diamidino-2-phenylindole (DAPI) in VECTASHIELD® Mounting Medium, H-1200 (Vector Laboratories, Burlingame, CA). A TUNEL assay for histological section was carried out using paraformaldehyde-fixed mouse tissues.

For the PCNA assay, tissue sections were incubated with PBS containing 0.3% $H_2O_2$ for 30 min at room temperature. The sections were then incubated with biotin-conjugated anti-PCNA antibody (1:1000) with 3% BSA in PBS overnight at 4 °C. The sections were then incubated in series with streptavidin-HRP diluted with 3% BSA in PBS (1:1000) and 3,3′-diaminobenzidine tetrahydrochloride (DAB) choromogen (Dako, Kyoto, Japan). The sections were counterstained with Mayer's hematoxylin and examined by light microscopy.

*Statistical Analysis*—Data are expressed as the means ± S.E. of the mean. Comparisons were made using the two-tailed Stu-

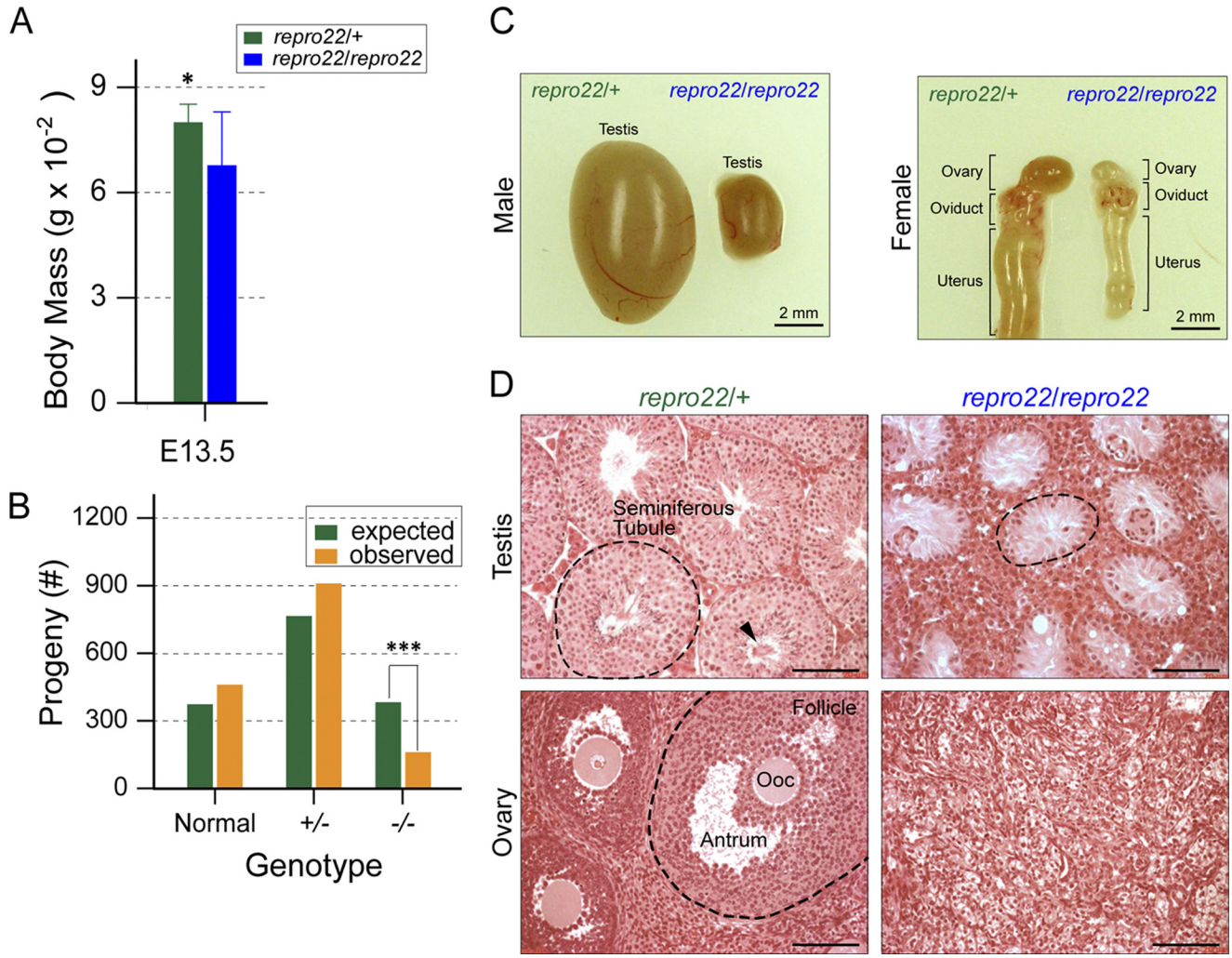


FIGURE 1. **Morphology and histology of *repro22/repro22* gonads.** *A*, comparison of body weights between *repro22/+* and *repro22/repro22* mice at E13.5. The embryos show significant reduction in body size. Values represent the means ± S.E. ($n = 5$) and were statistically different at $p < 0.03$. *B*, the genotype of ~1500 progeny from *repro22/+* heterozygous parents varied from expected Mendelian inheritance ($p < 0.001$). *C*, *repro22/+* and *repro22/reprod22* testes and female reproductive tracts from 8-week-old mice. *D*, section of testes and ovaries from 16-week-old *repro22/+* and *repro22/repro22* mice were stained with hematoxylin-eosin. The *arrowhead* points to the lumen in a normal seminiferous tubule. *Scale bar*, 100 μm. *Ooc*, oocyte.

dent's test (*t* test), $X^2$, or analysis of variance and considered highly significant with *p* values of ≤0.01 and significant with *p* values of ≤0.05. The *p* values and significance levels are described in the figure legends.

## RESULTS

*Growth Retardation and Increased Embryonic Lethality of Homozygous repro22 Mice*—During our initial analyses of homozygous *repro22* mice, we found decreased size and body weight in adult mice of both genders compared with those of normal littermates. These differences were evident as early as E7.5 and E8.5 and persisted from birth into adulthood, suggesting that the genetic defect in *repro22* mice causes severe growth retardation in prenatal development (Fig. 1*A*). We also found that a significant number of homozygous mutant animals died during embryogenesis. Analysis of 1511 $F_2$ offspring from intercrosses of *repro22/+* mice indicated a dramatically reduced number of affected mice. The distortion from Mendelian ratio with no sex ratio distortion suggested an autosomal single recessive mode of inheritance with partial lethality. The progeny data indicated that only ~40% of affected animals survived after weaning (Fig. 1*B*), and both male and female mice were strikingly sterile.

*Defective Development of PGCs in repro22 Mice*—At 8 weeks of age, the male and female gonads of *repro22* mice were ~10% the size of those of normal mice (Fig. 1*C*). Examining gonadal histology, we observed complete absences of germ cells in male and female mice. Although testicular tubules were formed, they lacked germ cells, and neither follicles nor germ cells were present in adult ovaries (Fig. 1*D*). The documented absence of germ cells in adults of both sexes suggested a common defect in prenatal germ cell development. In mice, PGCs first appear in the developing gonad at E7.25 and are defined by their large size and strong alkaline phosphatase activity (28, 34). Therefore, we examined the developmental process of PGCs in affected and normal mouse embryos from E7.5 to E13.5 using alkaline phosphatase staining of gonadal sections and whole-mount embryos. The presence of pre-migratory PGCs in the hindgut pocket of affected and normal mice at E8.5 suggested that specification and initial formation of PGCs were not significantly

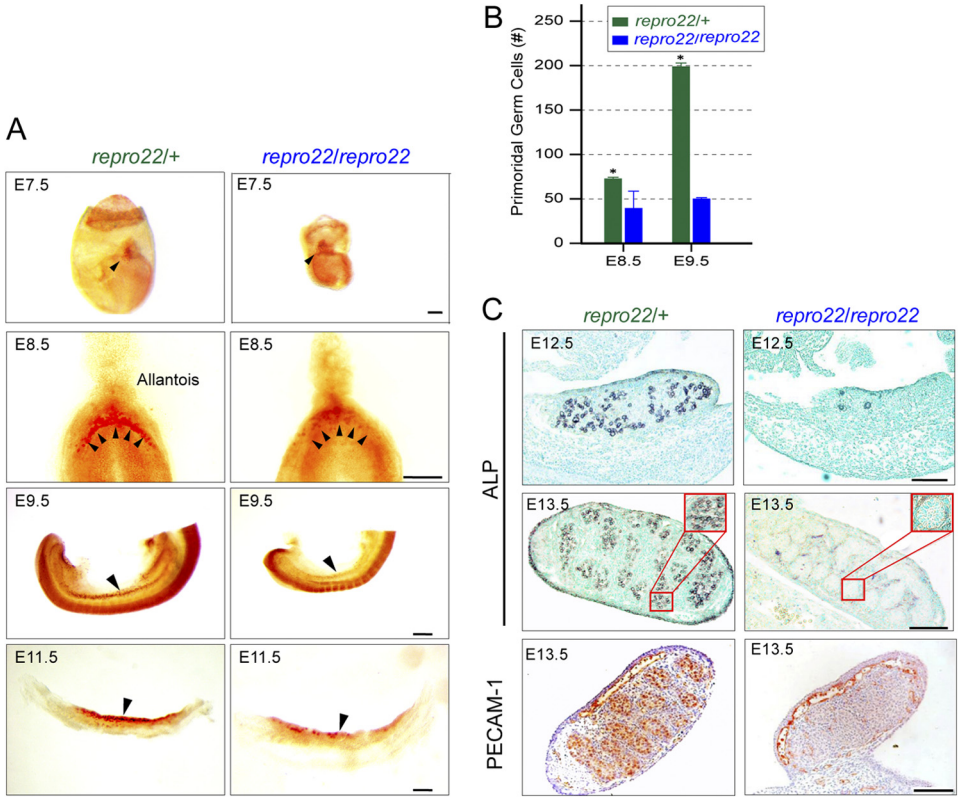


FIGURE 2. **Germ cell loss and embryonic defects in *repro22*/*repro22* mice during embryonic development.** *A*, whole-mount embryo and genital ridge preparations of *repro22*/+ and *repro22*/*repro22* embryos were isolated at embryonic day E7.5, E8.5, E9.5, and E11.5 and stained with alkaline phosphatase (*ALP*). *Arrowheads* point to PGCs. *B*, the number of PGCs in *repro22*/+ and *repro22*/*repro22* mice at E8.5 ($n = 3$) and E9.5 ($n = 4$) quantified from serial sections of embryonic gonads. Values represent the means ± S.E. and were statistically different at $p < 0.05$. *C*, embryonic gonads (XY, E12.5 and E13.5) from *repro22*/+ and *repro22*/*repro22* mice isolated and stained with alkaline phosphatase or PECAM-1 to detect PGCs. *Scale bar*, 100 μm.

affected in *repro22* mutant mice (Fig. 2*A*). In addition, PGCs were not significantly decreased in *repro22* embryos at E7.25 compared with those in normal embryos (Fig. 2*A*), suggesting normal PGC specification in *repro22* mice. However, the number of PGCs in the affected mice was approximately half that of normal mice at E8.5, and the differences became more pronounced in the hindgut mesentery at E9.5 and in the genital ridges at E11.5 (Fig. 2*B*). Notably, although fewer in number, PGCs in *repro22* mice did successfully arrive and colonize the genital ridges at E11.5, suggesting that the defect in the mutant mouse is not in migration but in proliferation and survival of PGCs or both (Fig. 2*A*).

The widening difference in cell number persisted in E12.5 gonads, and at E13.5, when normal gonads were fully populated, few or no PGCs were detected in the mutant gonad either by alkaline phosphatase staining or PCAM1 immunostaining (Fig. 2*C*). We observed no differences in testicular cord formation, which was comparable with that of normal male gonads. Taken together, these observations during PGC development suggested that both defects in proliferation and survival of PGCs during PGCs development account for germ cell depletion in affected adult male and female mice. These findings in PGC development as well as growth retardation and partial lethality of the mutant mouse suggested that the mutated gene in *repro22* mice has an essential role in proliferation and survival of both somatic and germ cells during development.

*Fine Mapping and Positional Cloning of the repro22 Locus*—The *repro22* mutant locus had been mapped initially to a 13-Mb region between *D4Mit57* and *D4Mit42* on the distal end of chromosome 4 (The Jackson Laboratory). To refine the location of the mutation, we determined the genotypes of microsatellite markers (Table 1) in this region in 160 affected mice (320 meiotic events) of 1511 $F_2$ offspring from intercrosses of C57BL/6 and JF1/Ms mice as well as C57BL/6 and C3H/HeJ strains. No recombination between *repro22* and *D4Mok5* or *D4Mok6* was observed, but one to four recombination events between *repro22* and the other eight microsatellite markers were present. These data refined the critical region to a 70-kb interval between *D4Mok3* and *D4Mok7* markers (Fig. 3*A*), which included a cluster of three *F-box* genes (*Fbox2*, *Fbox4*, and *Fbox6*), one EST(*2610109H07Rik*), and *Rev7* (Fig. 3 B).

We determined the coding sequence of all of these genes in affected and normal mice by sequencing cDNA derived from various tissues. No functional mutation or nucleotide difference specific to the affected animals was observed in *Fbox2*, *Fbox4*, *Fbox6*, or *2610109H07Rik* genes. However, in *Rev7*, we identified a single nucleotide substitution of T to C at nucleotide 208 in the coding region, which resulted in an amino acid substitution of Cys to Arg at codon 70 (C70R) in a highly conserved region of the HORMA domain, which is implicated in chromatin binding (Fig. 3, *C* and *D*). The complete association between the missense mutation and the *repro22* phenotype in the $F_2$ progeny was observed with PCR-RFLP analysis using BstuI endonuclease, and this allele was absent in various inbred strains (Fig. 3*E*). These findings indicated that the C70R muta-

**TABLE 1**
**Sequences of PCR primers and expected size of amplified fragments**

| Markers | Primers | | Size |
|---|---|---|---|
| | Forward (5′-3′) | Reverse (5′-3′) | |
| | | | bp |
| *D4mit233* | CCCACCCCACTCATCATAAA | AGGAGAGCCAGAGCTACACAA | 167 |
| *D4Mit285* | CTTTAGGTAGAACTTCTTCCGTTTT | GTGGCAGTGAAACTTATTCAACC | 100 |
| *D4Nimr1* | AGGGAATCTGATGCCTTTGC | TCAGTAAGTGTGCTTGCCTG | 220 |
| *D4Mok3* | AAACTGCAAGGGACACCATC- | GCAACAGGCTAGAGCCAGAC | 183 |
| *D4Mok4* | TGTATGTGTGTAGCCATGAATTT | GGCCTCATGATGCTAAGGAA | 150 |
| *D4Mok5* | TATGTCCCCTGTCCCCTACC | CCCAGCCCTGTCTTTTTCTT | 184 |
| *D4Mok6* | TGTAGGTCTTTTCTCATTTACGTG | AACTTCCAGGACCCATTGAG | 150 |
| *D4Mok7* | GCTTCCTCCCTGAACACAGT | AGCACATCTCTGTGGGTGTG | 192 |
| *D4Mok8* | GCCCGGTTAAACCTGACTTT | CCAACACCTTCTGGCCTCT | 226 |
| *D4Mit127* | GTGTGCTGATGCAGGCAC | GAGAGGAATGCTGGTAGGCA | 145 |
| *Mad2l2* | GGTTGCCTTGAGTCCCTACAG | GTAGTGGGACAGCTGGGTAGC | 728 |
| *Mad2l2* | TGTGTGTGGGTTATTGCTGTT | AGGCTTCTGGCTGTTGAAAG | 239 |

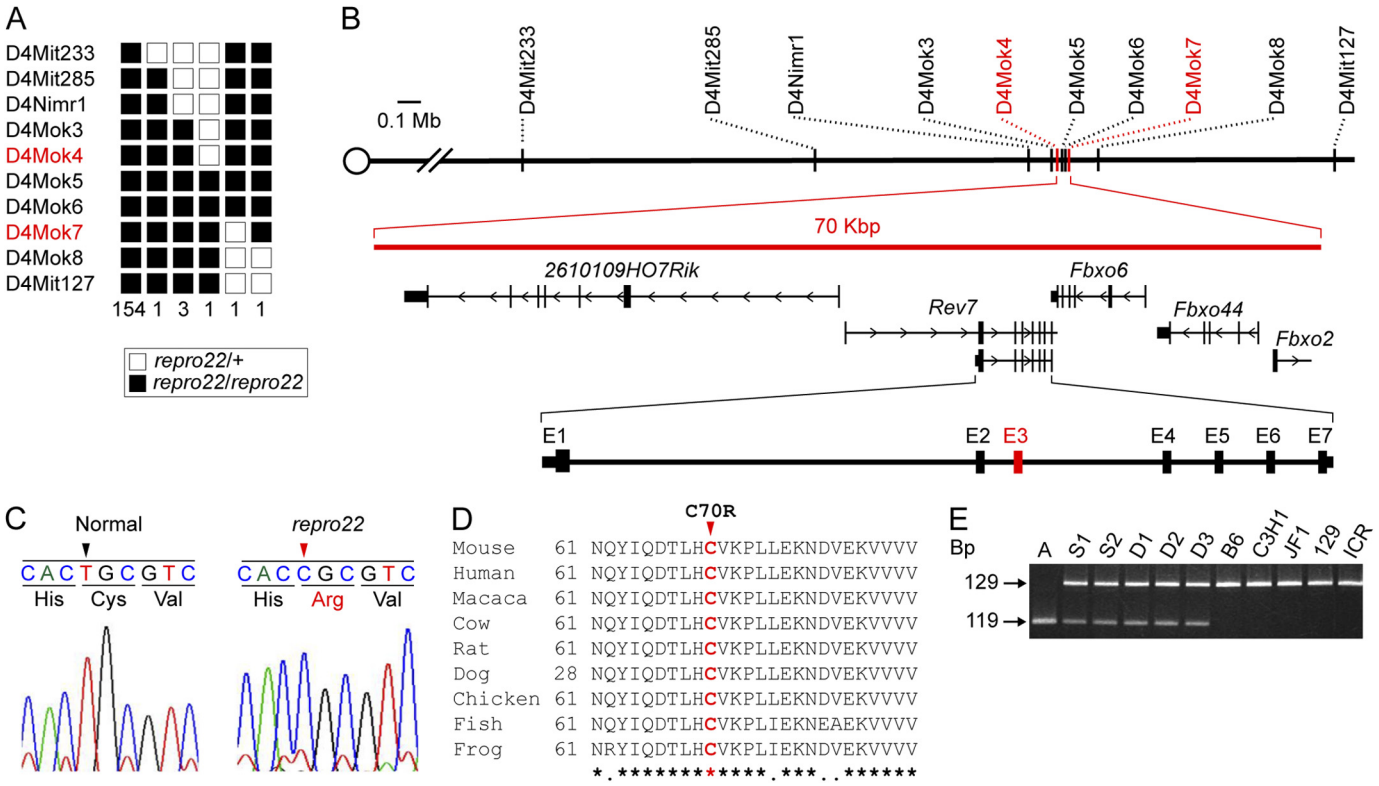


FIGURE 3. **Molecular characterization of the *repro22* mutation.** *A*, segregation of haplotypes in 160 affected $F_2$ mice. The number of mice for each haplotype is indicated at the *bottom of the columns*. *B*, localization of microsatellite markers, positions, and transcriptional orientations of three genes and an expressed sequence tag in the interval defined in *A*. An exon map of *Rev7* is indicated at the *bottom*. *C*, nucleotide sequence of normal and *repro22* alleles showing nucleotide substitution of T to C that results in missense mutation of Cys to Arg. *D*, alignment of the deduced amino acid sequences in the HORMA domain of vertebrate REV7 in which Cys-70 is well conserved. *E*, RFLP analysis of the specificity of the mutant allele using BstUI restriction enzyme in affected (*A*), parental heterozygous animals (*S1*, *S2*, *D1*, *D2*, and *D3*) and several inbred strains of mice.

tion of *Rev7* was responsible for germ cell depletion in *repro22/repro22* mice.

*Transgenic Rescue*—To confirm that the $Rev7^{C70R}$ mutation was responsible for germ cell depletion in $Rev7^{C70R/C70R}$ mice, we performed genetic complementation by establishing transgenic mice with a genomic fragment containing the normal *Rev7* gene. A 24.8-kb genomic fragment containing the entire coding region and the predicted 5′ regulatory region of *Rev7* was isolated from a BAC clone and injected into mouse oocytes via intracytoplasmic sperm injection-mediated transgenesis (Fig. 4, *A* and *B*). Mice with the *Rev7* transgene were crossed with *repro22*/+ mice and subsequently intercrossed with $Rev7^{TG/+}$;$Rev7^{C70R/+}$ mice to produce $Rev7^{TG/+}$;$Rev7^{C70R/C70R}$ transgenic mice (Fig. 4*C*). Analysis of developing PGCs at E12.5 documented that the genital ridges of the $Rev7^{TG/+}$;$Rev7^{C70R/C70R}$ mice were as full of alkaline phosphatase-positive PGCs as those in normal control mice (Fig. 4*D*). Fertility was fully restored in both male and female $Rev7^{TG/+}$;$Rev7^{C70R/C70R}$ mice, and the size of their testes and ovaries were normal. On histological examination, the seminiferous tubules of the $Rev7^{TG/+}$;$Rev7^{C70R/C70R}$ mice were filled with germ cells including spermatogonia, spermatocytes, spermatozoa, and mature spermatids, and the ovaries contained multiple follicles with oocytes at various stages of development as well as corpora lutea (Fig. 4*E*). No histological difference was observed

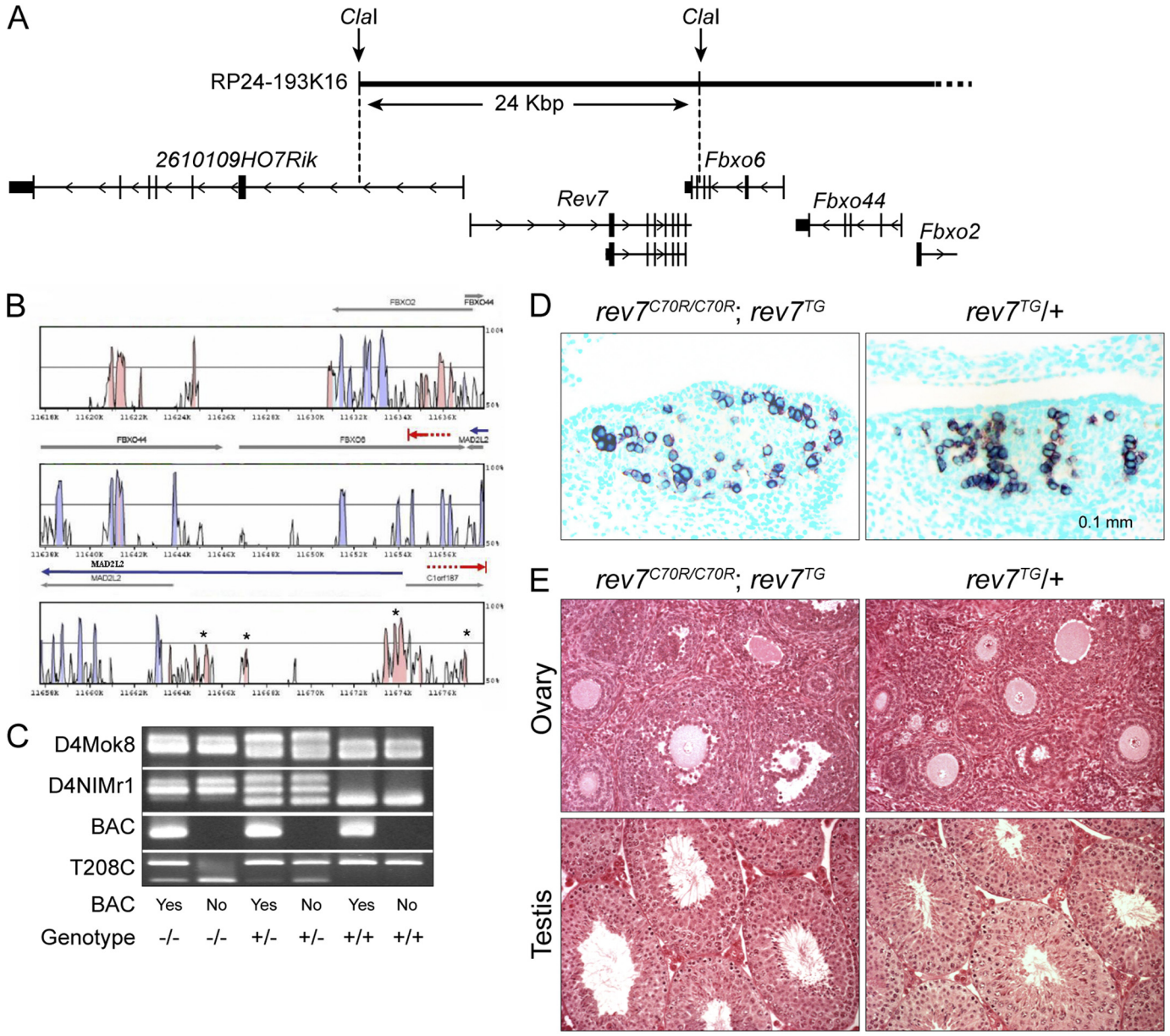


FIGURE 4. **Rescue of *Rev7*$^{C70R}$ mutant mice by a *Rev7* transgenic line.** *A*, schematic representation of BAC clone RP24–193K16 containing *Rev7* and three other genes. The clone was digested using ClaI restriction enzyme to isolate a 24.8-kb fragment containing the entire *Rev7* gene including 5 kb of the potential regulatory 5′ region and a 3-kb 3′ untranslated region of the gene. *B*, comparative analysis of mouse and human *Rev7* genomic regions using the VISTA program (26) to identify potential regulatory regions of the gene (*pink columns marked with asterisks*). *C*, genotyping of *Rev7*$^{TG}$/+;*Rev7*$^{C70R/C70R}$ rescue mice using two microsatellite markers flanking the *repo22* region, T208C allele RFLP, and a 130-bp PCR fragment to determine the *Rev7*$^{TG}$ allele. *D*, alkaline phosphatase (*ALP*) staining of XX gonads at E12.5 in *Rev7*$^{TG}$/+ and *Rev7*$^{C70R/C70R}$;*Rev7*$^{TG}$ mice documents complete rescue of PGC proliferation. *E*, hematoxylin-eosin staining of testis and ovary from *Rev7*$^{TG}$/+ and *Rev7*$^{C70R/C70R}$;*Rev7*$^{TG}$ mice (7 weeks old) confirms that the *Rev7* transgenic mouse can fully rescue *Rev7*$^{C70R/C70R}$ mice.

between the testes or ovaries of normal and *Rev7*$^{TG/+}$; *Rev7*$^{C70R/C70R}$ mice. Therefore, the *repro22* phenotypes were completely rescued by *Rev7*$^{TG}$, demonstrating that the loss of function mutation of *Rev7*$^{C70R}$ is responsible for germ cell depletion in *Rev7*$^{C70R/C70R}$ mice.

*Expression Analysis of Rev7 in PGCs and Adult Tissues*—Based on alkaline phosphatase staining in *Rev7*$^{C70R}$ mutant mice, defects in PGCs were first apparent in the gonad at E8.5 and culminated with near complete loss of germ cells by E13.5. We, therefore, assessed the expression of the *Rev7* gene during the proliferative stage of PGC development using FACS sorting of β-galactosidase-tagged PGCs (30). *Rev7* expression in both male and female gonads was detected from E7.5 to E13.5 but not at E14.5 when the proliferative phase of PGCs was complete in male and female mice. Although a single transcript predominated during embryonic development, three additional isoforms of *Rev7* were present; particularly at E11.5, two variant transcripts specific to female PGCs were observed (Fig. 5 A). We confirmed that these variants are alternatively spliced isoforms caused by skipping of exons 2 and/or 4 by sequencing of these transcripts.

We also examined expression of *Rev7* in various tissues of adult mouse. As shown in Fig. 5*B*, *Rev7* expressed ubiquitously in many tissues and highest expression was observed in testis. It

is to be noted that the expression of the *Rev7* transcripts is also observed in tissues of *Rev7*$^{C70R/C70R}$ mice (Fig. 5*B*), indicating that the C70R mutation does not affect the level of *Rev7* expression. The observed elimination of *Rev7* expression in the mutant testis could be due to the absence of the germ cells in the mutant testis.

*Effects of the Rev7 Mutation on Somatic Cells*—The ubiquitous expression of *Rev7* suggested that that REV7 functions not only germ cells but also in various types of somatic cells, and the defects of REV7 could result in defective proliferation of somatic cells as observed in the germ cells. We, therefore, examined growth of MEFs isolated from normal, *Rev7*$^{C70R/+}$, and *Rev7*$^{C70R/C70R}$ mouse embryos. As shown in Fig. 6*A*, the growth ratio C70R/C70R MEF was significantly lower than that of normal MEFs at 48 h of culture. These findings indicated that the defect of REV7 affects the proliferation of somatic cells.

Next, we examined *in vivo* effects of the *Rev7* mutation on somatic cells. Because the effects of the *Rev7* mutation are expected to be more apparent in rapidly proliferating cells, we assessed ratios of growth and apoptosis in intestinal epithelial cells. As shown in Fig. 6, *B* and *C*, the numbers of PCNA-positive S-phase cells were not significantly different between normal and *Rev7*$^{C70R/C70R}$ mice. However the number of TUNEL-positive cells in *Rev7*$^{C70R/C70R}$ mice was significantly increased, and the number of epithelial cells in each villus was significantly reduced in *Rev7*$^{C70R/C70R}$ mice. These findings indicated that the *Rev7* mutation results in growth defects of intestinal epithelial cells by an increased number of apoptotic cells.

*Defects in Spindle Assembly Checkpoint Function Do Not Account for the repro22 Phenotype*—REV7/MAD2L2 is homologous to the MAD2 protein, which is a key component of the mitotic spindle assembly checkpoint. Thus, *Rev7*/*Mad2l2* might also regulate cell cycle progression as an arbiter of the spindle assembly checkpoint and could contribute to the growth retardation and germ cell depression observed in *Rev*$^{C70R}$ mutant mice. To test this possibility, we treated *Rev7*$^{C70R/C70R}$ MEF with colcemid and harvested the cells hourly over 8 h. The cells were fixed and stained with phosphohistone H3 (Ser-10) antibody, a marker of mitosis, and the mitotic index was measured for each genotype (11, 35). We observed increased cell arrest at mitosis in the presence of colcemid in all genotypes (Fig. 7*A*) without significant difference. We conclude that that *Rev7*$^{C70R}$ is unlikely to be involved in the regulation of the spindle assembly checkpoint.

*Rev7*$^{C70R}$ *Disrupts Interaction with REV3*—Therefore, we focused on the possibility that the *Rev7*$^{C70R}$ mutation affects

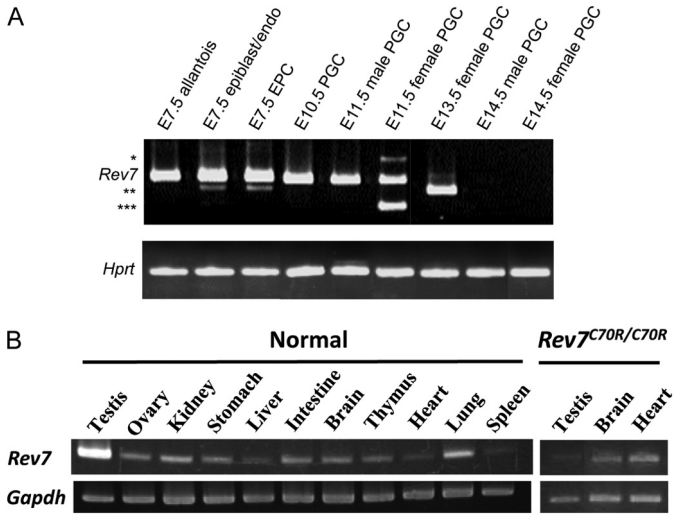


FIGURE 5. **Expression of *Rev7* in germ cells and adult tissues.** *A*, expression of *Rev7* was detected by RT-PCR in FACS-sorted PGCs from E10.5 to E14.5 and at the base of the allantois (E7.5) consisting of both somatic and nascent PGCs. *B*, expression analysis of *Rev7* in adult tissues by RT-PCR show ubiquitous expression of *Rev7* in normal and *Rev7*$^{C70R/C70R}$ mouse. Expressions of *Gapdh* were shown as the control.

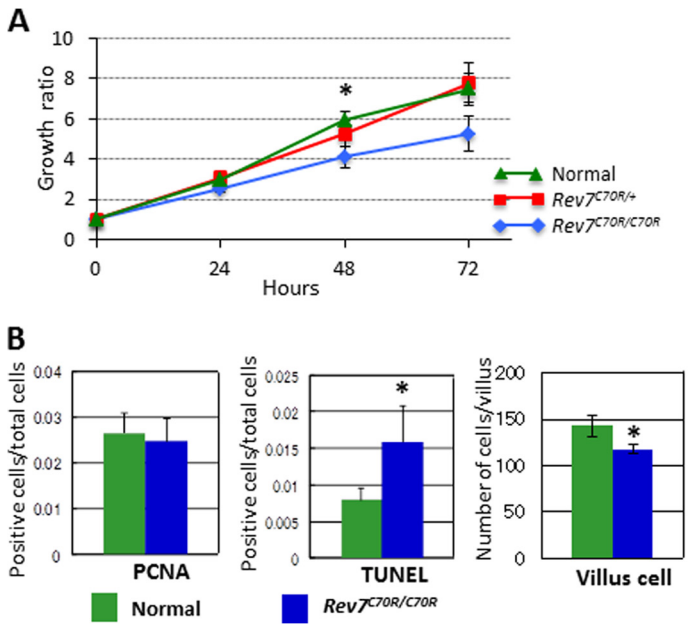


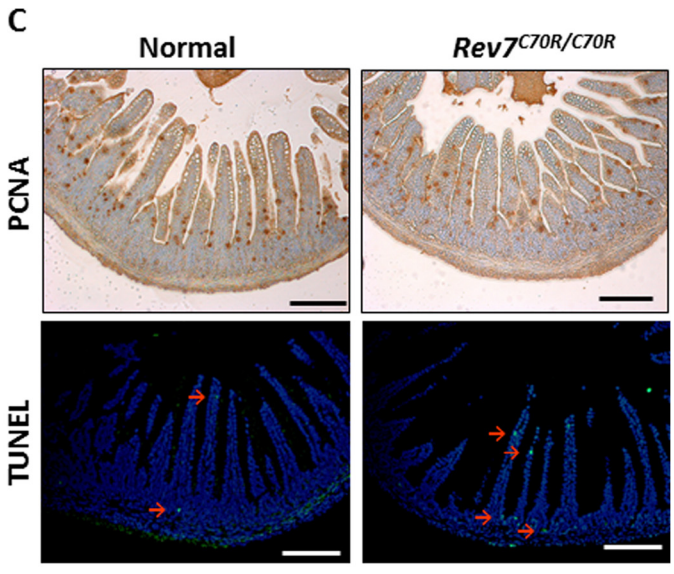


FIGURE 6. **Effects of *Rev7*$^{C70R}$ mutation on growth of somatic cells.** *A*, growth ratios of normal, *Rev7*$^{C70R/+}$, and *Rev7*$^{C70R/C70R}$ MEFs show a significant difference between normal and *Rev7*$^{C70R/C70R}$ MEFs at 48 h of culture indicating reduced growth of *Rev7*$^{C70R/C70R}$ cells. *B* and *C*, numbers of PCNA-positive cells, TUNEL-positive cells, and cells in each villus of normal ($n = 3$) and *Rev7*$^{C70R/C70R}$ ($n = 3$) mice indicate increased apoptotic cells and growth defects in *Rev7*$^{C70R/C70R}$ intestinal epithelial cells. *, $p < 0.05$. *Scale bar*, 100 $\mu$m.

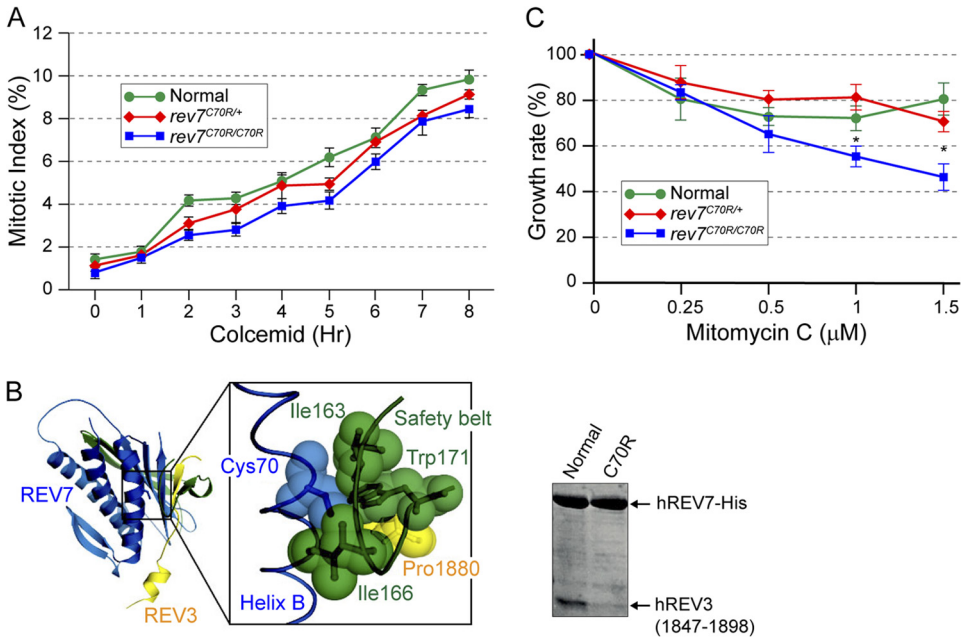


FIGURE 7. ***Rev7*$^{C70R}$ mutation disrupts DNA polymerase/(Polζ) formation and sensitizes cells to ICL agents.** *A*, mitotic index in normal, *Rev7*$^{C70R/+}$, and *Rev7*$^{C70R/C70R}$ cells at different time points after treatment with colcemid showed no significant differences among the genotypes. *B*, *in vitro* interaction assay between REV7 and REV3 fragments. In contrast to normal REV7, the C70R substitution of REV7 impairs REV3 binding. The detailed structure around Cys-70 of REV7 in the REV7-REV3 complex in which REV7 is *blue* and *green* (safety belt) and the REV3 fragment is *yellow* indicates that Cys-70 interacts with Ile-163, Ile-166, and Trp-171 of the safety belt, which are adjacent to Pro-1880 of REV3. The figures were produced by the structural data of REV7-REV3(1847–1898) complex (PDB ID 3ABD) (31). *C*, reduced growth rate of *Rev7*$^{C70R/C70R}$ mutant cells compared with *Rev7*$^{C70R/+}$ or normal cells after treatment with mitomycin C (0.25–1.50 μm). *hRev7-His*, human *Rev7-His*. Values represent the means ± S.E. ($n = 6$) and were statistically different at $p < 0.02$.

interactions with REV3, the catalytically active subunit of DNA Polζ, and affects TLS activity of the cell. The crystal structure of human REV7 in complex with the REV3 fragment documents that Cys-70 contacts Ile-163, Ile-166, and Trp-171 of REV7, which is adjacent to Pro-1880 of REV3 (Fig. 7*B*). Thus, the C70R mutation of REV7 would significantly perturb the interaction between Trp-171 of REV7 and Pro-1880 of REV3, which is crucial for REV7-REV3 interaction, and the C70R mutation could disrupt the formation of DNA Polζ. To confirm whether C70R disrupts REV7-REV3 interactions, we examined the interaction of REV7 with the REV3 fragment using an *in vitro* binding assay (Fig. 7*B*). The mutant REV7 protein with C70R bound little if at all to the REV3$^{1847-1898}$ fragment, whereas normal REV7 protein showed a strong signal for binding to the REV3$^{1847-1898}$ fragment. Thus, we conclude that the *Rev7*$^{C70R}$ mutation significantly impairs REV3 interactions that form the DNA Polζ complex, resulting in defective TLS activity.

*Rev7*$^{C70R}$ *Mutation Sensitizes Embryonic Cells to ICL Agents*—The *Rev* family of proteins is uniquely associated with protection against cisplatin- and mitomycin C-induced DNA damage and repair of ICL in human cells as well as in chicken DT40 cell lines (11, 36). We, therefore, investigated whether the *Rev7*$^{C70R}$ mutation sensitizes cells to a particular type of DNA damage similar to that observed in siRNA-directed knockdown of *REV7* in human (36) or nasopharyngeal carcinoma cells lines (37). Relative cell survival rates of normal, *Rev7*$^{C70R/+}$, and *Rev7*$^{C70R/C70R}$ MEFs were measured with microculture tetrazolium assays after treatment with various concentrations of mitomycin C. The cytotoxicity of mitomycin C is ascribed largely to its capability to generate ICLs in DNA (38). Unlike normal controls, *Rev7*$^{C70R}$ mutant cells were hypersensitive to ICL-inducing mitomycin C (Fig. 7*C*). These findings indicate that the disruption of *REV7/REV3* interaction caused by the *Rev7*$^{C70R}$ mutation increases the susceptibility of cells to agents that cause ICL damage.

*Analysis of γH2AX and 53BP1 Localization in Response to ICL Agents*—Because *Rev7*$^{C70R/C70R}$ cells showed significant sensitivity to DNA-damaging agents, we next investigated the efficiency of DNA repair systems in mutant cells under induced DNA damage. DNA damages, including DSB, can be visualized as subnuclear foci of γH2AX and/or 53BP1 protein. To determine whether the REV7 mutation induces the formation or persistence of DNA damages, we stained *Rev7*$^{C70R/C70R}$ and normal cells with antibodies to γH2AX and 53BP1. The γH2AX foci were dramatically increased in *Rev7*$^{C70R/C70R}$ cells. Cells were classified according to the number of γH2AX foci per nucleus, and when uniform staining of the entire nucleus without foci was observed, the cells were classified as displaying pan-nuclear (PN) staining (Fig. 8*A*). Although <20% of normal and *Rev7*$^{C70R/+}$ cells had PN staining, >60% of *Rev7*$^{C70R/C70R}$ cells had PN staining (Fig. 8*B*), indicating accumulated DNA damage in the mutant cells after mitomycin C treatment. As a result of increased ratio of PN staining, <20% of *Rev7*$^{C70R/C70R}$ nuclei showed 0–30 γH2AX foci, whereas ~50% of normal and *Rev7*$^{C70R/+}$ cells showed 0–30 γH2AX foci (Fig. 8*B*). Interestingly, when the cells were double-stained with antibodies to γH2AX and 53BP1, a significant portion of the γH2AX foci in nucleus with low density foci co-localized with 53BP1, but the PN-stained cells showed no 53BP1 co-localization (Fig. 8*C*). Because γH2AX is accumulated at the site DNA damages, including DSB and ICL, which cause stalling of replication fork, 53BP1 protein is mainly enriched at sites of DSB (39). Therefore, the PN staining of γH2AX

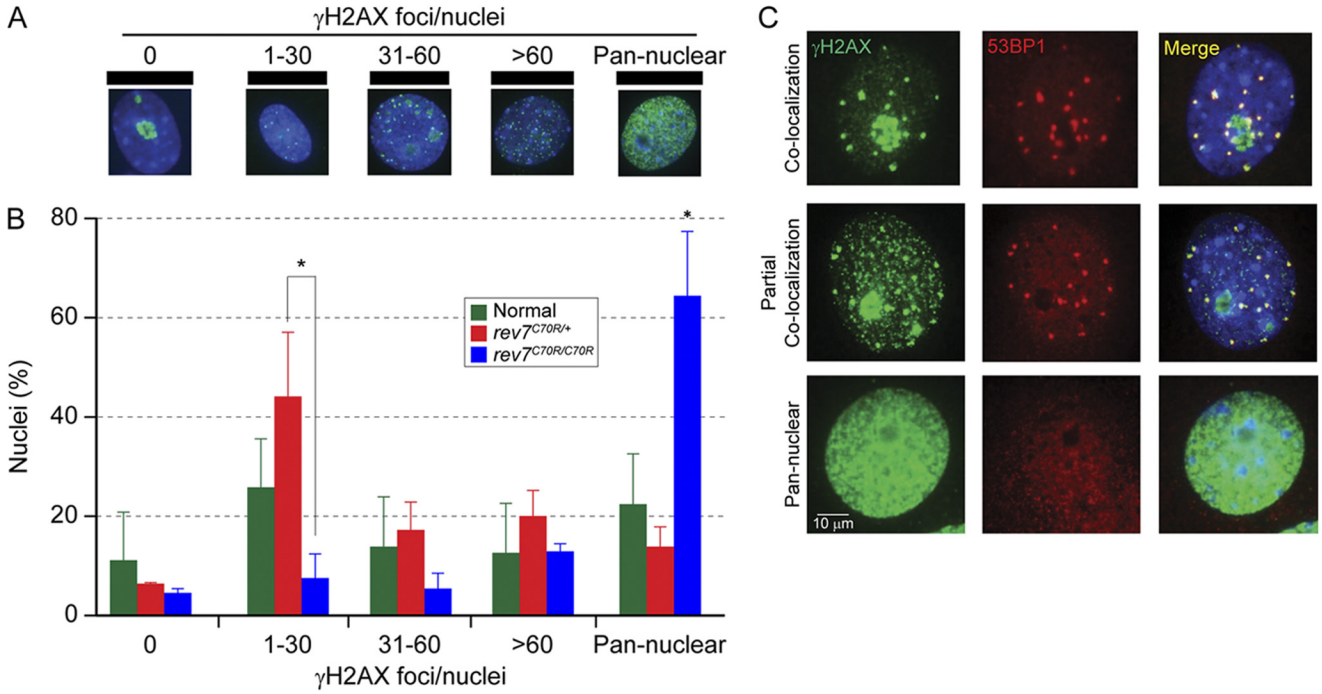


FIGURE 8. ***Rev7*$^{C70R/C70R}$ cells show widespread nuclear γH2AX staining.** *A*, levels of γH2AX staining were classified based on the number of γH2AX foci per nucleus and pan-nuclear staining. *B*, significant increase of pan-nuclear staining in *Rev7*$^{C70R/C70R}$ cells, which display replication-stalled nuclei, after treatment with mitomycin C. *C*, co-localization of γH2AX (*green*) and the DNA damage response protein 53BP1 (*red*) in *Rev7*$^{C70R/C70R}$ cells. The cells were treated with mitomycin C. Whereas a significant portion of the γH2AX foci in nucleus with low density foci co-localize with 53BP1, those with pan-nuclear staining are completely free of 53BP1 staining and represent replication-stalled cells at S phase.

without 53BP1 focus observed in the present study is suggested to represent replication fork stalling caused by ICL rather than DSB.

*Rev7 Is Required for S Phase Repair of ICL Damage*—To determine the cell cycle phase that requires DNA Polζ, we performed cytometry analysis in normal, *Rev7*$^{C70R/+}$, and *Rev7*$^{C70R/C70R}$ cells. MEFs were stained with γH2AX antibody and counterstained with propidium iodide to determine the cell cycle stage 16 and 48 h after mitomycin C treatment (33). Control cells from each genotype without mitomycin C treatment had weak or negative signals. However, a striking difference was observed after treatment with mitomycin C. At 16 h, a large number of cells with strong positive signals for γH2AX corresponding to PN staining was observed in all genotypes. Forty-eight hours after mitomycin C treatment, the number of strongly positive cells decreased dramatically in normal and *Rev7*$^{C70R/+}$ cells, indicating DNA repair and cell cycle resumption. However, *Rev7*$^{C70R/C70R}$ cells remained strongly positive for γH2AX staining, and the portion of cells in S phase was dramatically increased compared with that in normal cells (Fig. 9, *A* and *B*), indicating stalling of the cell cycle at S phase. An increased number of TUNEL-positive cells was also observed in *Rev7*$^{C70R/C70R}$ MEFs after mitomycin C treatment (Fig. 9*C*). Thus, in the absence of functional DNA Polζ, *Rev7*$^{C70R/C70R}$ cells do not undergo ICL repair, increasing apoptosis after mitomycin C treatment and suggesting hypersensitivity to ICL-inducing agents.

## DISCUSSION

Homozygous *reprod22* mice display growth retardation, germ cell depletion, and sterility. Using positional cloning, we characterized *repro22* as a C70R missense mutation in a highly conserved region of the HORMA (DNA binding) domain of the *Rev7* gene. Mouse *Rev7* has significant homology with yeast *rev7*, a member of the yeast *rev* family of genes including *rev1*, *rev3*, and *rev7*. The encoded REV7 protein interacts with REV3 to form DNA Polζ, a critical component of TLS (7, 40). The structure of human REV7 in complex with a REV3 fragment has been defined (32), and replacement of Cys-70 with Arg introduces an elongated and positively charged side chain predicted to interfere with normal interactions within the REV7 safety belt and prevent binding to REV3. This outcome was confirmed experimentally by the observation that REV3 bound to REV7, but not to *Rev7*$^{C70R}$, when co-expressed in bacteria. The REV7-REV3 interaction is indispensable for REV3 function (32). Thus, the *Rev7*$^{C70R}$ mutation is predicted to affect Polζ catalytic activity and prevent the TLS activity required to repair DNA damage and necessary to ensure cell cycle progression and proliferation during development. Beyond TLS activity, *Rev7* is widely accepted to be a multifunctional protein acting as an adaptor in various biological pathways. *Rev7* interacts with various proteins, including the *Shigella* effector IpaB in bacterial invasion of host cells, and is an activator of APC by interacting with Cdh1, Cdc20, or both (23). We examined whether *Rev7*$^{C70R}$ mutation displays defects in spindle assembly checkpoint function by treating the MEFs with colcemid and observed no difference between normal and *Rev7*$^{C70R/C70R}$ MEFs. Because colcemid is a microtubule-depolymerizing drug and could trigger the spindle assembly checkpoint, these data indicated no defect related to APC function of REV7.

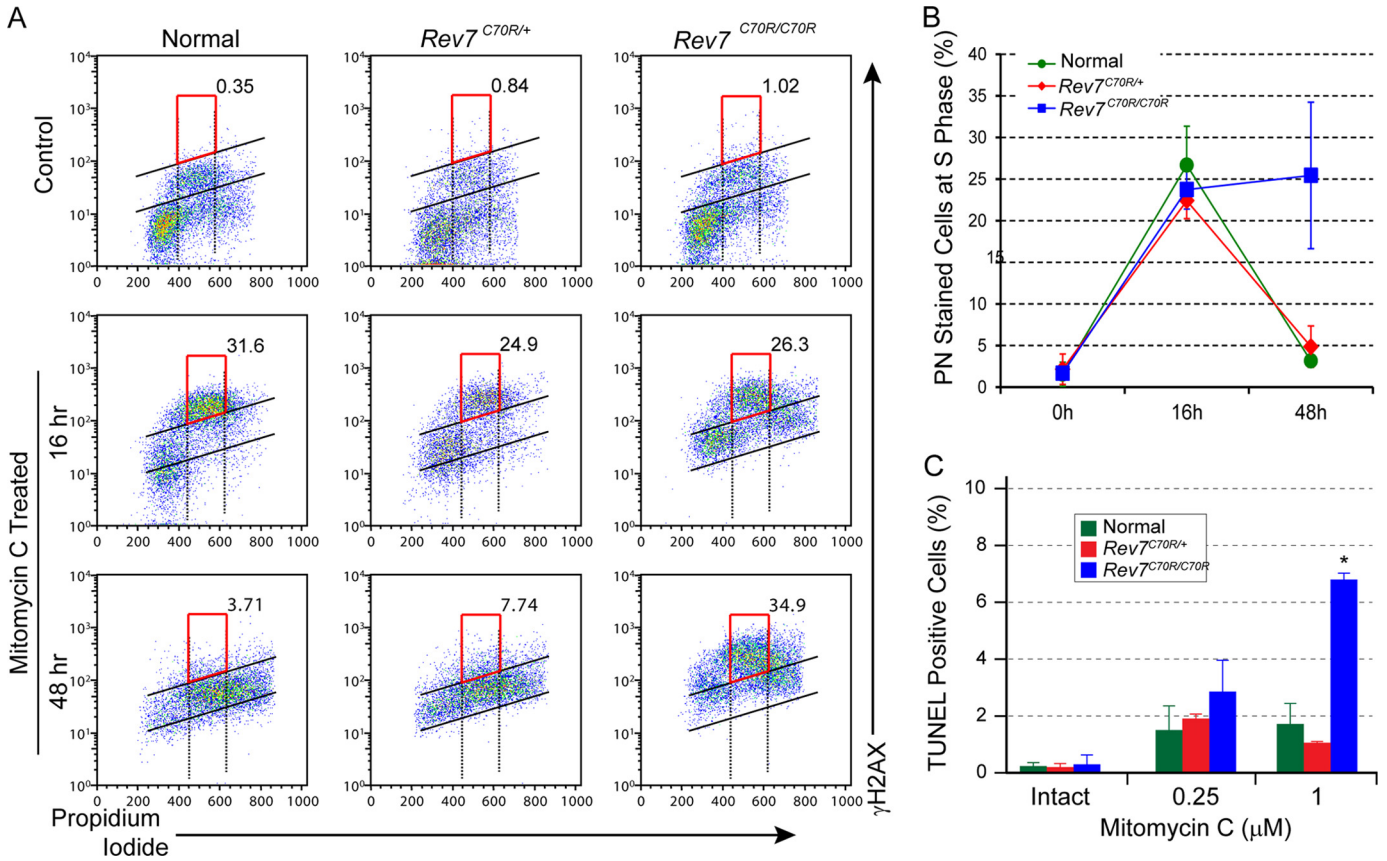


FIGURE 9. **Rev7 is required for S phase repair of ICL damage.** *A*, although mutant and normal cells show increased S phase accumulation of strong PN γH2AX staining at 16 h after mitomycin C treatment, only normal and $Rev7^{C70R/+}$ cells bypassed S phase at 48 h after mitomycin C treatment. The persistence of γH2AX staining in S phase nuclei documents the inability of $Rev7^{C70R/C70R}$ cells to bypass DNA damage. *Numbers* represent the percent of cells within the *red boxes*. *B*, the percentage of PN-stained cells is dramatically increased in MEFs of all genotypes at 16 h and decreased at 48 h in normal and $Rev7^{C70R/+}$ MEFs but not in $Rev7^{C70R/C70R}$ MEFs. Values represent mean percentages ± S.E. ($n = 3$) and were statistically different at $p < 0.01$. *C*, a significant increase of apoptotic cells was observed after mitomycin C treatment. Values represent mean percentages ± S.E. ($n = 3$) and were statistically different at $p < 0.05$.

A significant number of DNA lesions occur daily in every cell, and the majority of them stall DNA polymerases, resulting in DNA replication stress. As a curative measure, canonical polymerases can be replaced by TLS polymerases that are adapted to correct replicative defects including those arising as interstrand adducts. This formulation is consistent with our experimental observation that reduction of Polζ function in $Rev7^{C70R/C70R}$ cells leads to increased susceptibility to the DNA-damaging agent mitomycin C, which catalyzes ICL. Therefore, we conclude that the inability of $Rev7^{C70R/C70R}$ cells to correct DNA lesions resulted in DNA replication stress.

The repair of ICL is not well understood in mammals but involves a recombination-independent pathway in the $G_1$ phase and a replication- and recombination-dependent pathway in the S phase of the cell cycle (41, 42). The Fanconi anemia (FA) pathway plays a pivotal role in resolving ICL at S phase and acts upstream of TLS DNA polymerases (Fig. 8). The FA core complex contains an E3 ubiquitin ligase that is recruited to the DNA lesion. Mono-ubiquitination of FANCD2 and FANCI (FA II) coordinates endonucleolytic cleavage of the blocked replication fork followed by unhooking that leaves the cross-linked nucleotide tethered to the complementary strand that is then bypassed by TLS DNA polymerase (41–43). Polυ, Polθ, and Polζ have been implicated in these pathways (42), and reconstitution of ICL repair *in vitro* has documented that depletion of Polζ impairs the process in *Xenopus laevis* egg extracts (44). We found that $Rev7^{C70R/C70R}$ cells are hypersensitive to ICL agents, displaying increased DSBs and replication stalling in S phase. Involvement of Polζ in ICL repair has also been reported in HeLa cells using small interfering RNA technology (36). The processing of ICLs in $G_1$ phase involves nucleotide excision repair and endonucleolytic cleavage of ICL. In addition to the FA core complex, PCNA becomes mono-ubiquitinated in response to DNA damage, which allows loading of y-family TLS polymerases and bypass of the lesion followed by nucleotide excision repair of the damaged DNA (Fig. 8*A*) (43, 45). Whether $Rev7^{C70R}$ mutant cells bypass the $G_1$ phase of ICL repair is unknown. However, because Polκ is known as a primary participant in $G_1$ phase ICL DNA repair (46), $Rev7^{C70R}$ mutant cells are unlikely to have $G_1$ phase ICL repair defects caused by a lack of Polζ function in replication-independent ICL repair.

Among genetically targeted mice with germ cell depletion, mutations affecting the FA complex proteins FANCL, FANCC, and FANCA show phenotypes similar to those of $Rev7^{C70R}$ mice, with drastic reduction of germ cells proliferation and infertility (47–52). In particular, FancL mutant mice (51) and $Usp1^{-/-}$ $Fancd2^{-/-}$ double-mutant mice (52) show the most severe phenotypes similar to those observed in $Rev7^{C70R}$ mutant mice. Unlike $Rev7^{C70R}$, mutations in other TLS polymerases do not affect PGC development (53–58). In addition,

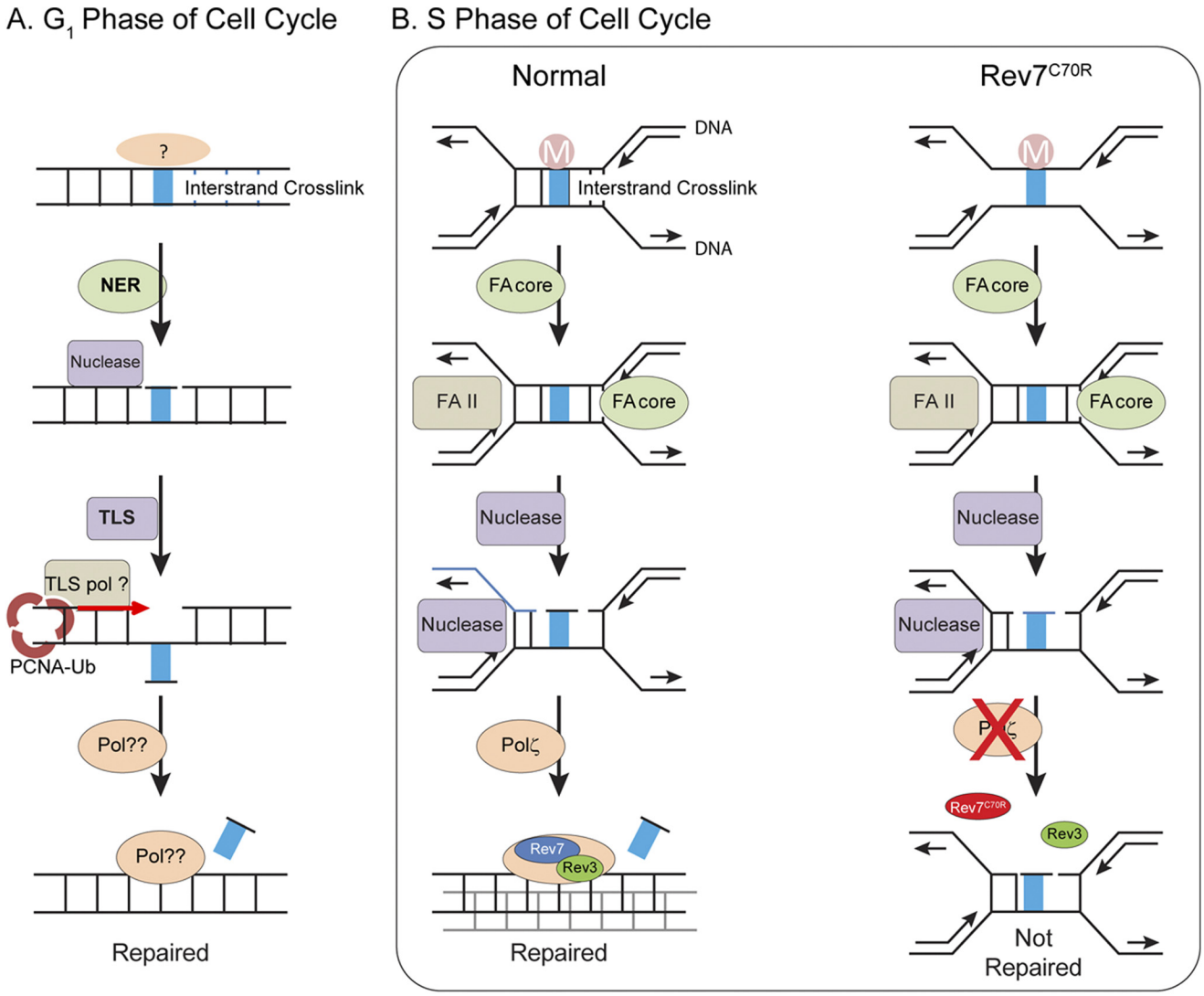


FIGURE 10. **Model describing requirement of *Rev7* in ICL repair.** *A*, processing of ICLs in the $G_1$ phase of the cell cycle involves nucleotide excision repair (*NER*) and endonucleolytic cleavage of ICL. PCNA becomes mono-ubiquitinated by E2 ubiquitin ligases in response to DNA damage, which allows loading of TLS polymerases and bypass of the lesion followed by nucleotide excision repair of the damaged DNA. *B*, in the S phase of the cell cycle, ICL repair requires an upstream FA pathway coupled to Polζ (*left panel*). FA core proteins are recruited by FANCM (*M*) to the ICL (*red bar*), which monoubiquitinates the FA-II complex followed by DNA incision and unhooking of the cross-linked DNA. On the incised strand, TLS polymerase is recruited to bypass the unhooked cross-link followed by nucleotide excision repair. However, the *Rev7*$^{C70R}$ mutation disrupts formation of Polζ, leading to incomplete DNA replication and persistence of S phase-stalled cells with double-strand breaks (*right panel*). Thus, Polζ is the TLS polymerase downstream of the FA pathway required to resolve ICL and relieve DNA replication arrest in S phase.

similar to cells with the *Rev7*$^{C70R}$ mutation, cells derived from FA and Usp1 null mutants are sensitive to ICL-inducing agents. Our data show that the lack of REV7 function results in accumulation of γH2AX without 53BP1 colocalization at S phase, which could represent unresolved replication-fork stalling caused by DNA damages (39). These findings indicated that S phase ICL repair requires *Rev7* and suggest that DNA Polζ functions downstream of the FA pathway. The more severe phenotypes of *Rev7*$^{C70R}$ mutant mice show that although some redundancy might occur in the FA and *Usp1* families of genes, the TLS polymerases downstream of these pathways are restricted to control by Polζ. Interestingly, other TLS polymerases, including Polκ, the primary participant in $G_1$ phase ICL DNA repair, showed neither defects related to fertility nor developmental defects.

A recently reported targeted mutation of *Rev7* (*Rev7*$^{KO}$) (59) shows phenotypes similar to those of *Repro22* mice, with growth retardation and embryonic loss of germ cells. That report and our own show lost PGCs during development from E8.5 to E13.5, reduced body size, and embryonic lethality. Moving beyond the common phenotypes observed in both cases and taking advantage of a point mutation in *Rev7*, we performed additional functional analysis of *Rev7*, the findings of which are summarized as below.

We studied formation of PGCs at E7.5 and observed that it is unaffected by *Rev7*$^{C70R}$ mutation, which demonstrates that *Rev7* is not involved in PGC formation. In addition, a previous study (59) could not show any clear expression of *Rev7* in PGCs during development. Instead, we isolated PGCs from both male and female embryos during development from E7.5to E14.5

and clearly show that *Rev7* is expressed during that period and that the expression was absent on E14.5 coincident with a well known PGC proliferation stage.

PGC development has three important steps, namely formation, migration, and proliferation. We found that the $Rev7^{C70R/C70R}$ cells are proliferation-deficient through three pieces of evidence obtained in the present study. First, accumulated cells arrested at S phase of the cell cycle and strongly expressed γH2AX and displayed widespread apoptosis. Second, although *Rev7* is expressed ubiquitously in various tissues, quiescent cells are not affected by the *Rev7* mutation; it affects mainly proliferative cells during embryonic development. Third, the expression pattern in PGC development is consistent with the well known period of proliferation between E7.5 and E13.5. The expression ceased on E14.5, when the proliferation of PGCs stopped in both male and female mice. Rather than the proposed defect in germ cell maintenance (34), our results with $Rev7^{C70R}$ mice indicate a defect in proliferation secondary to absent TLS activity. Consistent with our results, conditional targeting of *Rev3* in skin epithelia (60) does not affect survival but is essential for responses requiring rapid proliferation of epithelial cells. Also notable is that the present findings indicated decreased growth ratio of the $Rev7^{C70R}$ MEFs and increased apoptosis in $Rev7^{C70R}$ intestinal epithelial cells, which are among the most rapidly proliferating cells. These findings also support our hypothesis that the rev7 mutation mainly affects rapidly proliferating cells and accounts for growth retardation and increased embryonic lethality observed in $Rev7^{C70R/C70R}$ mice.

The point mutation of the $Rev7^{C70R}$ disrupts its interaction with *Rev3*, therefore, impairing Polζ formation. We next excluded the possibility that this point mutation might affect another proposed function of *Rev7* as an APC activator. We found that $Rev7^{C70R}$ mutant cells are hypersensitive to ICL agents and that ICL repair is abrogated at S phase in $Rev7^{C70R/C70R}$ cells, suggesting that ICL repair at this stage requires *Rev7* and Polζ. Interestingly, the phenotypes in *repro22* mice were similar to those of mice with mutations in the FA pathway. This pathway is well known for its function in replication-dependent ICL repair during S phase, which acts upstream of a TLS polymerase. We, therefore, show that the TLS polymerase required for replication-dependent ICL repair is Polζ.

Using the results of the present study, we proposed a model (Fig. 10) in which Polζ is required for ICL repair at S phase of the cell cycle and acts in concert and downstream of the FA pathway. $Rev7^{C70R/C70R}$ mice will provide an excellent model for investigation of the function of Polζ in genome stability in both somatic and germ cells.

*Acknowledgments—We thank Dr. J. Dean for critical discussions and editorial comments. We thank Drs. J. J. Eppig, M. A. Handel, and J. C. Schimenti for providing the repro22 mutant mice produced by the ReproGenomics Program at The Jackson Laboratory. We also thank Maho Maekawa for technical assistance.*

## REFERENCES

1. Lange, S. S., Takata, K., and Wood, R. D. (2011) DNA polymerases and cancer. *Nat. Rev. Cancer* **11,** 96–110
2. Loeb, L. A., and Monnat, R. J., Jr. (2008) DNA polymerases and human disease. *Nat. Rev. Genet.* **9,** 594–604
3. Saribasak, H., Maul, R. W., Cao, Z., Yang, W. W., Schenten, D., Kracker, S., and Gearhart, P. J. (2012) DNA polymerase ζ generates tandem mutations in immunoglobulin variable regions. *J. Exp. Med.* **209,** 1075–1081
4. Daly, J., Bebenek, K., Watt, D. L., Richter, K., Jiang, C., Zhao, M. L., Ray, M., McGregor, W. G., Kunkel, T. A., and Diaz, M. (2012) Altered Ig hypermutation pattern and frequency in complementary mouse models of DNA polymerase ζ Activity. *J. Immunol.* **188,** 5528–5537
5. Friedberg, E. C., Lehmann, A. R., and Fuchs, R. P. (2005) Trading places. How do DNA polymerases switch during translesion DNA synthesis? *Mol. Cell* **18,** 499–505
6. Gan, G. N., Wittschieben, J. P., Wittschieben, B. Ø., and Wood, R. D. (2008) DNA polymerase ζ (pol ζ) in higher eukaryotes. *Cell Res.* **18,** 174–183
7. Aravind, L., and Koonin, E. V. (1998) The HORMA domain. A common structural denominator in mitotic checkpoints, chromosome synapsis, and DNA repair. *Trends Biochem. Sci.* **23,** 284–286
8. Takata, K., and Wood, R. D. (2009) Bypass specialists operate together. *EMBO J.* **28,** 313–314
9. Gibbs, P. E., McGregor, W. G., Maher, V. M., Nisson, P., and Lawrence, C. W. (1998) A human homolog of the *Saccharomyces cerevisiae* REV3 gene, which encodes the catalytic subunit of DNA polymerase ζ. *Proc. Natl. Acad. Sci. U.S.A.* **95,** 6876–6880
10. Morrison, A., Christensen, R. B., Alley, J., Beck, A. K., Bernstine, E. G., Lemontt, J. F., and Lawrence, C. W. (1989) REV3, a *Saccharomyces cerevisiae* gene whose function is required for induced mutagenesis, is predicted to encode a nonessential DNA polymerase. *J. Bacteriol.* **171,** 5659–5667
11. Okada, T., Sonoda, E., Yoshimura, M., Kawano, Y., Saya, H., Kohzaki, M., and Takeda, S. (2005) Multiple roles of vertebrate REV genes in DNA repair and recombination. *Mol. Cell. Biol.* **25,** 6103–6111
12. Sharma, S., Hicks, J. K., Chute, C. L., Brennan, J. R., Ahn, J. Y., Glover, T. W., and Canman, C. E. (2012) REV1 and polymerase ζ facilitate homologous recombination repair. *Nucleic Acids Res.* **40,** 682–691
13. Wittschieben, J. P., Reshmi, S. C., Gollin, S. M., and Wood, R. D. (2006) Loss of DNA polymerase ζ causes chromosomal instability in mammalian cells. *Cancer Res.* **66,** 134–142
14. Esposito, G., Godindagger, I., Klein, U., Yaspo, M. L., Cumano, A., and Rajewsky, K. (2000) Disruption of the Rev3l-encoded catalytic subunit of polymerase ζ in mice results in early embryonic lethality. *Curr. Biol.* **10,** 1221–1224
15. Wittschieben, J., Shivji, M. K., Lalani, E., Jacobs, M. A., Marini, F., Gearhart, P. J., Rosewell, I., Stamp, G., and Wood, R. D. (2000) Disruption of the developmentally regulated Rev3l gene causes embryonic lethality. *Curr. Biol.* **10,** 1217–1220
16. Bemark, M., Khamlichi, A. A., Davies, S. L., and Neuberger, M. S. (2000) Disruption of mouse polymerase ζ (Rev3) leads to embryonic lethality and impairs blastocyst development *in vitro*. *Curr. Biol.* **10,** 1213–1216
17. Schenten, D., Kracker, S., Esposito, G., Franco, S., Klein, U., Murphy, M., Alt, F. W., and Rajewsky, K. (2009) Pol ζ ablation in B cells impairs the germinal center reaction, class switch recombination, DNA break repair, and genome stability. *J. Exp. Med.* **206,** 477–490
18. Wittschieben, J. P., Patil, V., Glushets, V., Robinson, L. J., Kusewitt, D. F., and Wood, R. D. (2010) Loss of DNA polymerase ζ enhances spontaneous tumorigenesis. *Cancer Res.* **70,** 2770–2778
19. Lange, S. S., Wittschieben, J. P., and Wood, R. D. (2012) DNA polymerase ζ is required for proliferation of normal mammalian cells. *Nucleic Acids Res.* **40,** 4473–4482
20. Rimkus, C., Friederichs, J., Rosenberg, R., Holzmann, B., Siewert, J. R., and Janssen, K. P. (2007) Expression of the mitotic checkpoint gene MAD2L2 has prognostic significance in colon cancer. *Int. J. Cancer* **120,** 207–211
21. Pfleger, C. M., Salic, A., Lee, E., and Kirschner, M. W. (2001) Inhibition of Cdh1-APC by the MAD2-related protein MAD2L2. A novel mechanism for regulating Cdh1. *Genes Dev.* **15,** 1759–1764
22. Chen, J., and Fang, G. (2001) MAD2B is an inhibitor of the anaphase-promoting complex. *Genes Dev.* **15,** 1765–1770
23. Iwai, H., Kim, M., Yoshikawa, Y., Ashida, H., Ogawa, M., Fujita, Y., Muller, D., Kirikae, T., Jackson, P. K., Kotani, S., and Sasakawa, C. (2007) A bacte-

rial effector targets Mad2L2, an APC inhibitor, to modulate host cell cycling. *Cell* **130,** 611–623
24. Lessard, C., Lothrop, H., Schimenti, J. C., and Handel, M. A. (2007) Mutagenesis-generated mouse models of human infertility with abnormal sperm. *Hum. Reprod.* **22,** 159–166
25. Abbasi, A. R., Khalaj, M., Tsuji, T., Tanahara, M., Uchida, K., Sugimoto, Y., and Kunieda, T. (2009) A mutation of the WFDC1 gene is responsible for multiple ocular defects in cattle. *Genomics.* **94,** 55–62
26. Couronne, O., Poliakov, A., Bray, N., Ishkhanov, T., Ryaboy, D., Rubin, E., Pachter, L., and Dubchak, I. (2003) Strategies and tools for whole-genome alignments. *Genome. Res.* **13,** 73–80
27. Perry, A. C., Wakayama, T., Kishikawa, H., Kasai, T., Okabe, M., Toyoda, Y., and Yanagimachi, R. (1999) Mammalian transgenesis by intracytoplasmic sperm injection. *Science* **284,** 1180–1183
28. Lawson, K. A., Dunn, N. R., Roelen, B. A., Zeinstra, L. M., Davis, A. M., Wright, C. V., Korving, J. P., and Hogan, B. L. (1999) Bmp4 is required for the generation of primordial germ cells in the mouse embryo. *Genes Dev.* **13,** 424–436
29. Ginsburg, M., Snow, M. H., and McLaren, A. (1990) Primordial germ cells in the mouse embryo during gastrulation. *Development* **110,** 521–528
30. Abe, K., Hashiyama, M., Macgregor, G., and Yamamura, K. i. (1996) Purification of primordial germ cells from TNAP$\beta$-geo mouse embryos using FACS-gal. *Dev. Biol.* **180,** 468–472
31. Hara, K., Shimizu, T., Unzai, S., Akashi, S., Sato, M., and Hashimoto, H. (2009) Purification, crystallization, and initial X-ray diffraction study of human REV7 in complex with a REV3 fragment. *Acta Crystallogr. Sect. F. Struct. Biol. Cryst. Commun.* **65,** 1302–1305
32. Hara, K., Hashimoto, H., Murakumo, Y., Kobayashi, S., Kogame, T., Unzai, S., Akashi, S., Takeda, S., Shimizu, T., and Sato, M. (2010) Crystal structure of human REV7 in complex with a human REV3 fragment and structural implication of the interaction between DNA polymerase $\zeta$ and REV1. *J. Biol. Chem.* **285,** 12299–12307
33. Huang, X., and Darzynkiewicz, Z. (2006) Cytometric assessment of histone H2AX phosphorylation. A reporter of DNA damage. *Methods Mol. Biol.* **314,** 73–80
34. Lawson, K. A., and Hage, W. J. (1994) Clonal analysis of the origin of primordial germ cells in the mouse. *Ciba Found. Symp.* **182,** 68–84
35. Saeki, A., Tamura, S., Ito, N., Kiso, S., Matsuda, Y., Yabuuchi, I., Kawata, S., and Matsuzawa, Y. (2002) Frequent impairment of the spindle assembly checkpoint in hepatocellular carcinoma. *Cancer* **94,** 2047–2054
36. Hicks, J. K., Chute, C. L., Paulsen, M. T., Ragland, R. L., Howlett, N. G., Guéranger, Q., Glover, T. W., and Canman, C. E. (2010) Differential roles for DNA polymerases eta, $\zeta$, and REV1 in lesion bypass of intrastrand *versus* interstrand DNA cross-links. *Mol. Cell. Biol.* **30,** 1217–1230
37. Cheung, H. W., Chun, A. C., Wang, Q., Deng, W., Hu, L., Guan, X. Y., Nicholls, J. M., Ling, M. T., Chuan Wong, Y., Tsao, S. W., Jin, D. Y., and Wang, X. (2006) Inactivation of human MAD2B in nasopharyngeal carcinoma cells leads to chemosensitization to DNA-damaging agents. *Cancer Res.* **66,** 4357–4367
38. Kratz, K., Schöpf, B., Kaden, S., Sendoel, A., Eberhard, R., Lademann, C., Cannavó, E., Sartori, A. A., Hengartner, M. O., and Jiricny, J. (2010) Deficiency of FANCD2-associated nuclease KIAA1018/FAN1 sensitizes cells to interstrand crosslinking agents. *Cell* **142,** 77–88
39. de Feraudy, S., Revet, I., Bezrookove, V., Feeney, L., and Cleaver J. E. (2010) A minority of foci or pan-nuclear apoptotic staining of $\gamma$H2AX in the S phase after UV damage contain DNA double-strand breaks. *Proc. Natl. Acad. Sci. U.S.A.* **107,** 6870–6875
40. Murakumo, Y., Ogura, Y., Ishii, H., Numata, S., Ichihara, M., Croce, C. M., Fishel, R., and Takahashi, M. (2001) Interactions in the error-prone postreplication repair proteins hREV1, hREV3, and hREV7. *J. Biol. Chem.* **276,** 35644–35651
41. Deans, A. J., and West, S. C. (2011) DNA interstrand crosslink repair and cancer. *Nat. Rev. Cancer* **11,** 467–480
42. Ho, T. V., and Schärer, O. D. (2010) Translesion DNA synthesis polymerases in DNA interstrand crosslink repair. *Environ. Mol. Mutagen.* **51,** 552–566
43. Wang, W. (2007) Emergence of a DNA-damage response network consisting of Fanconi anaemia and BRCA proteins. *Nat. Rev. Genet.* **8,** 735–748
44. Räschle, M., Knipscheer, P., Knipsheer, P., Enoiu, M., Angelov, T., Sun, J., Griffith, J. D., Ellenberger, T. E., Schärer, O. D., and Walter, J. C. (2008) Mechanism of replication-coupled DNA interstrand crosslink repair. *Cell* **134,** 969–980
45. Chun, A. C., and Jin, D. Y. (2010) Ubiquitin-dependent regulation of translesion polymerases. *Biochem. Soc. Trans.* **38,** 110–115
46. Williams, H. L., Gottesman, M. E., and Gautier, J. (2012) Replication-independent repair of DNA interstrand crosslinks. *Mol. Cell* **47,** 140–147
47. Moldovan, G. L., and D'Andrea, A. D. (2009) How the fanconi anemia pathway guards the genome. *Annu. Rev. Genet.* **43,** 223–249
48. Chen, M., Tomkins, D. J., Auerbach, W., McKerlie, C., Youssoufian, H., Liu, L., Gan, O., Carreau, M., Auerbach, A., Groves, T., Guidos, C. J., Freedman, M. H., Cross, J., Percy, D. H., Dick, J. E., Joyner, A. L., and Buchwald, M. (1996) Inactivation of Fac in mice produces inducible chromosomal instability and reduced fertility reminiscent of Fanconi anaemia. *Nat. Genet.* **12,** 448–451
49. Wong, J. C., Alon, N., Mckerlie, C., Huang, J. R., Meyn, M. S., and Buchwald, M. (2003) Targeted disruption of exons 1 to 6 of the Fanconi Anemia group A gene leads to growth retardation, strain-specific microphthalmia, meiotic defects, and primordial germ cell hypoplasia. *Hum. Mol. Genet.* **12,** 2063–2076
50. Nadler, J. J., and Braun, R. E. (2000) Fanconi anemia complementation group C is required for proliferation of murine primordial germ cells. *Genesis* **27,** 117–123
51. Agoulnik, A. I., Lu, B., Zhu, Q., Truong, C., Ty, M. T., Arango, N., Chada, K. K., and Bishop, C. E. (2002) A novel gene, Pog, is necessary for primordial germ cell proliferation in the mouse and underlies the germ cell deficient mutation, gcd. *Hum. Mol. Genet.* **11,** 3047–3053
52. Kim, J. M., Parmar, K., Huang, M., Weinstock, D. M., Ruit, C. A., Kutok, J. L., and D'Andrea, A. D. (2009) Inactivation of murine Usp1 results in genomic instability and a Fanconi anemia phenotype. *Dev. Cell* **16,** 314–320
53. Shima, N., Munroe, R. J., and Schimenti, J. C. (2004) The mouse genomic instability mutation chaos1 is an allele of Polq that exhibits genetic interaction with Atm. *Mol. Cell. Biol.* **24,** 10381–10389
54. Desiderio, S. V., Yancopoulos, G. D., Paskind, M., Thomas, E., Boss, M. A., Landau, N., Alt, F. W., and Baltimore, D. (1984) Insertion of N regions into heavy-chain genes is correlated with expression of terminal deoxytransferase in B cells. *Nature* **311,** 752–755
55. Bertocci, B., De Smet A., Berek, C., Weill, J. C., and Reynaud, C. A. (2003) Immunoglobulin $\kappa$ light chain gene rearrangement is impaired in mice deficient for DNA polymerase mu. *Immunity* **19,** 203–211
56. Delbos, F., De Smet A., Faili, A., Aoufouchi, S., Weill, J. C., and Reynaud, C. A. (2005) Contribution of DNA polymerase eta to immunoglobulin gene hypermutation in the mouse. *J. Exp. Med.* **201,** 1191–1196
57. McDonald, J. P., Frank, E. G., Plosky, B. S., Rogozin, I. B., Masutani, C., Hanaoka, F., Woodgate, R., and Gearhart, P. J. (2003) 129-derived strains of mice are deficient in DNA polymerase $\iota$ and have normal immunoglobulin hypermutation. *J. Exp. Med.* **198,** 635–643
58. Schenten, D., Gerlach, V. L., Guo, C., Velasco-Miguel, S., Hladik, C. L., White, C. L., Friedberg, E. C., Rajewsky, K., and Esposito, G. (2002) DNA polymerase $\kappa$ deficiency does not affect somatic hypermutation in mice. *Eur. J. Immunol.* **32,** 3152–3160
59. Watanabe, N., Mii, S., Asai, N., Asai, M., Niimi, K., Ushida, K., Kato, T., Enomoto, A., Ishii, H., Takahashi, M., and Murakumo, Y. (2013) The REV7 subunit of DNA polymerase $\zeta$ is essential for primordial germ cell maintenance in the mouse. *J. Biol. Chem.* **288,** 10459–10471
60. Lange, S. S., Bedford, E., Reh, S., Wittschieben J. P., Carbajal, S., Kusewitt, D. F., DiGiovanni, J., and Wood, R. D. (2013) Dual role for mammalian DNA polymerase $\zeta$ in maintaining genome stability and proliferative responses. *Proc. Natl. Acad. Sci. U.S.A.* **110,** E687–E696